REPORT DOCUMENTATION PAGE

Form Approved OMB NO. 0704-0188

1. REPORT DATE (DD-MM-YYYY)	2. REPORT TYPE	3. DATES COVERED (From - To)
18-05-2023	Final Report	1-May-2019 - 30-Sep-2022

4. TITLE AND SUBTITLE
Final Report: Non-Hermitian Interactions in Photonics

5a. CONTRACT NUMBER
W911NF-19-1-0249

5b. GRANT NUMBER

5c. PROGRAM ELEMENT NUMBER
611102

6. AUTHORS

5d. PROJECT NUMBER

5e. TASK NUMBER

5f. WORK UNIT NUMBER

7. PERFORMING ORGANIZATION NAMES AND ADDRESSES

University of Pennsylvania
Office of Research Services
3451 Walnut Street, 5th Floor
Philadelphia, PA 19104 -6205

8. PERFORMING ORGANIZATION REPORT NUMBER

9. SPONSORING/MONITORING AGENCY NAME(S) AND ADDRESS (ES)

U.S. Army Research Office
P.O. Box 12211
Research Triangle Park, NC 27709-2211

10. SPONSOR/MONITOR'S ACRONYM(S)
ARO

11. SPONSOR/MONITOR'S REPORT NUMBER(S)
74453-PE.9

12. DISTRIBUTION AVAILIBILITY STATEMENT

Approved for public release; distribution is unlimited.

13. SUPPLEMENTARY NOTES

The views, opinions and/or findings contained in this report are those of the author(s) and should not contrued as an official Department of the Army position, policy or decision, unless so designated by other documentation.

14. ABSTRACT

15. SUBJECT TERMS

16. SECURITY CLASSIFICATION OF:			17. LIMITATION OF ABSTRACT	15. NUMBER OF PAGES	19a. NAME OF RESPONSIBLE PERSON
a. REPORT	b. ABSTRACT	c. THIS PAGE			Liang Feng
UU	UU	UU	UU		19b. TELEPHONE NUMBER 215-898-7106

RPPR Final Report
as of 25-May-2023

Agency Code: 21XD

Proposal Number: 74453PE **Agreement Number: W911NF-19-1-0249**
INVESTIGATOR(S):

Name: Liang Feng
Email: fenglia@seas.upenn.edu
Phone Number: 2158987106
Principal: Y

Organization: **University of Pennsylvania**
Address: Office of Research Services, Philadelphia, PA 191046205
Country: USA
DUNS Number: 042250712 EIN: 231352685

Report Date: 31-Dec-2022 Date Received: 18-May-2023
Final Report for Period Beginning 01-May-2019 and Ending 30-Sep-2022
Title: Non-Hermitian Interactions in Photonics
Begin Performance Period: 01-May-2019 **End Performance Period:** 30-Sep-2022
Report Term: 0-Other

Submitted By: Liang Feng Email: fenglia@seas.upenn.edu
Phone: (215) 898-7106

Distribution Statement: 1-Approved for public release; distribution is unlimited.

STEM Degrees: 2 **STEM Participants:** 9

Major Goals: The objective of this project is to investigate new types of optical interactions and couplings based on the synergy of two emerging fields of non-Hermitian photonics and topological physics.

Non-Hermitian Hamiltonians are in principle very general and their resulting interactions can be judiciously designed extremely versatile, shaping the symmetry and topology of exotic light states in photonic systems. To further promote the scope of non-Hermitian photonics, we aim here to develop a general fundamental framework for exploring and discovering different types of non-Hermiticity mediated novel interactions beyond recently studied parity-time symmetry, enabling new paradigms for dynamic control of light-matter interactions at micro- and nanoscale for innovative photonics symmetry and topology.

The intellectual merit of this proposed activity is based upon very recent developments of non-Hermitian and topological photonics that make use of powerful concepts of symmetry and topology — the two-guiding principles for understanding and synthesizing new phases of light in artificial materials, not available in nature. Although the connections between non-Hermitian and topological photonics are rather vague since they are emerging from different aspects of quantum physics, we propose to develop a fundamental framework to initiate the effective coupling of these two important yet different areas through different types of non-Hermitian interactions, including active controllable topological interaction, imaginary gauge field, and its resulting unidirectional coupling, as well as arbitrary complex-valued photonic couplings. These new types of non-Hermitian interactions will deliver novel active and reconfigurable photonics functionality ranging from topological insulating phases, and chiral resonances, to the dynamical control of lasers.

In the proposed project, we conduct basic theoretical studies, extensive numerical modeling and design, state-of-the-art fabrication, and characterization of the non-Hermitian photonic structures, facilitating efficient strategies to manipulate optical modes and enhance the robustness of light transport and cavity resonance using non-Hermitian interactions. The proposed studies are based on our recent theoretical and experimental studies of parity-time symmetric photonics, topological photonics, integrated photonics, and semiconductor optoelectronics. The project focused on the following three major research thrusts:

In Research Thrust I, we focused on non-Hermitian interaction for active control of the topological insulating phase, where the gain and loss in the system are strategically employed to reconfigure the topological order and thus the light routing pathways.

In Research Thrusts II, we concentrated on non-Hermitian interaction through an imaginary valued gauge field that

has no counterpart in condensed matter physics. We demonstrated an actively controlled gauge field and its governed robust chiral lasing and light transport.

In Research Thrust III, we studied the non-Hermitian interaction through an optical reservoir.

Accomplishments: In this project, we have substantial accomplishments across all three proposed thrusts:

Thrust I:
We have successfully demonstrated non-Hermitian topological light steering to flexibly route the optical signal. Flexible reconfiguration of topological pathways can enable a completely new paradigm for high-density photonics routing. However, the desired topological robustness, unfortunately, backfires to destroy the hope of topological tunability. To overcome this fundamental limitation, we perform non-Hermitian symmetry to enable a new kind of topological state into the bulk of the topological insulator with a uniform topology, for the first time. Without "battling" against topological protection, the new non-Hermitian topological states facilitate robust transmission links in the entire footprint to route optical signals to any desired output port. The ports-to-footprint ratio is at least two orders of magnitude higher than the state-of-the-art.

Thrust II:
We accomplished, for the first time, the non-Hermitian gauge field by employing the III-V semiconductor platform. By selectively patterning the pumping region, we are able to generate the desired gain/loss distribution for the imaginary-valued gauge field. Such a non-Hermitian gauge and its chiral properties can be actively controlled and switched, enabling a new class of reconfigurable chiral photonic components. By leveraging this actively controlled non-Hermitian gauge field, we have demonstrated cascaded tunable topological charge vortex microlasers. Moreover, we have demonstrated ultrafast control of the non-Hermitian gauge field and thus the ultrafast control of orbital angular momentum of laser emission on a picosecond scale.

We further developed the actively controlled non-Hermitian gauge to allow for simultaneous manipulations of both amplitude and phase, by which we demonstrated a hyperdimensional spin-orbit microlaser for chip-scale flexible generation and manipulation of arbitrary four-level states. Two microcavities coupled through a non-Hermitian synthetic gauge field are designed to emit spin-orbit-coupled states of light with six degrees of freedom. The vectorial state of the emitted laser beam in free space can be mapped on a Bloch hypersphere defining an SU(4) symmetry, demonstrating dynamical generation and reconfiguration of high-dimensional superposition states with high fidelity.

Thrust III:
We have demonstrated a higher-dimensional supersymmetric microlaser array where dissipative superpartners act as photonic reservoirs to couple to the main array. Through the dissipative couplings except for the fundamental supermode, high-power, single-frequency, small-divergence laser emission was demonstrated.

Training Opportunities: Nothing to Report

Results Dissemination: We have published 7 papers, including 4 in Science, 1 in Nature, 1 in PRL, and 1 in Light Science and Applications. All of them received wide international recognition. Many other scientific professional journals, websites, and news outlets reported this work in English and other languages (such as Spanish, German, and Chinese), including Nature Physics, Physics World, Physics Today, Phys.org, IEEE Spectrum, and so on. PI Feng and students have also presented the results in invited university seminars and conference talks (such as CLEO, APS March Meetings, and IEEE Photonics Conference).

Honors and Awards: Liang Feng:
2020 S. Reid Warren, Jr. Award by SEAS, University of Pennsylvania
2020 Italia Award – Aspen Institute
2020 Sloan Research Fellow
2019 Fellow of the Optical Society of America

Protocol Activity Status:

Technology Transfer: Patent applications:

Liang Feng and Han Zhao, Topological Photonic N×N Switch; U.S. Pat. Appl. No. 62/899,451, filed on September 12, 2019.

Liang Feng, Xingdu Qiao, Bikashkali Midya, Zihe Gao, High-Dimensional Evanescently Coupled Phase-Locked Microlaser Arrays; International Patent Application No. PCT/US2022/071817, filed on April 20, 2022; US Application No. 63/177,680, filed on April 21, 2021.

Liang Feng, Zhifeng Zhang, Haoqi Zhao, Li, Ge, Hyperdimensional spin-orbit microlaser; filed on November 16, 2022.

PARTICIPANTS:

Participant Type: PD/PI
Participant: Liang Feng
Person Months Worked: 3.00 **Funding Support:**
Project Contribution:
National Academy Member: N

Participant Type: Postdoctoral (scholar, fellow or other postdoctoral position)
Participant: Zihe Gao
Person Months Worked: 12.00 **Funding Support:**
Project Contribution:
National Academy Member: N

Participant Type: Graduate Student (research assistant)
Participant: Tianwei Wu
Person Months Worked: 15.00 **Funding Support:**
Project Contribution:
National Academy Member: N

Participant Type: Graduate Student (research assistant)
Participant: Xingdu Qiao
Person Months Worked: 12.00 **Funding Support:**
Project Contribution:
National Academy Member: N

Participant Type: Graduate Student (research assistant)
Participant: Wanying Ge
Person Months Worked: 6.00 **Funding Support:**
Project Contribution:
National Academy Member: N

RPPR Final Report
as of 25-May-2023

International Collaboration:

ITA

ARTICLES:

Publication Type: Journal Article Peer Reviewed: Y **Publication Status:** 1-Published
Journal: Science
Publication Identifier Type: DOI Publication Identifier: 10.1126/science.aay1064
Volume: 365 Issue: 6458 First Page #: 1163
Date Submitted: 8/13/20 12:00AM Date Published: 9/1/19 4:00AM
Publication Location:
Article Title: Non-Hermitian topological light steering
Authors: Han Zhao, Xingdu Qiao, Tianwei Wu, Bikashkali Midya, Stefano Longhi, Liang Feng
Keywords: Non-Hermitian, topological
Abstract: Photonic topological insulators provide a route for disorder-immune light transport, which holds promise for practical applications. Flexible reconfiguration of topological light pathways can enable high-density photonics routing, thus sustaining the growing demand for data capacity. By strategically interfacing non-Hermitian and topological physics, we demonstrate arbitrary, robust light steering in reconfigurable non-Hermitian junctions, in which chiral topological states can propagate at an interface of the gain and loss domains. Our non-Hermitian–controlled topological state can enable the dynamic control of robust transmission links of light inside the bulk, fully using the entire footprint of a photonic topological insulator.
Distribution Statement: 2-Distribution Limited to U.S. Government agencies only; report contains proprietary info
Acknowledged Federal Support: **Y**

Publication Type: Journal Article Peer Reviewed: Y **Publication Status:** 1-Published
Journal: Science
Publication Identifier Type: DOI Publication Identifier: 10.1126/science.aba8996
Volume: 368 Issue: 6492 First Page #: 760
Date Submitted: 8/13/20 12:00AM Date Published: 5/1/20 4:00AM
Publication Location:
Article Title: Tunable topological charge vortex microlaser
Authors: Zhifeng Zhang, Xingdu Qiao, Bikashkali Midya, Kevin Liu, Jingbo Sun, Tianwei Wu, Wenjing Liu, Ritesh
Keywords: orbital angular momentum, non-Hermitian symmetry
Abstract: Applications that use the orbital angular momentum (OAM) of light show promise for increasing the bandwidth of optical communication networks. However, direct photocurrent detection of different OAM modes has not yet been demonstrated. Most studies of current responses to electromagnetic fields have focused on optical intensity–related effects, but phase information has been lost. In this study, we designed a photodetector based on tungsten ditelluride (WTe_2) with carefully fabricated electrode geometries to facilitate direct characterization of the topological charge of OAM of light. This orbital photogalvanic effect, driven by the helical phase gradient, is distinguished by a current winding around the optical beam axis with a magnitude proportional to its quantized OAM mode number. Our study provides a route to develop on-chip detection of optical OAM modes, which can enable the development of next-generation photonic circuits.
Distribution Statement: 2-Distribution Limited to U.S. Government agencies only; report contains proprietary info
Acknowledged Federal Support: **Y**

RPPR Final Report
as of 25-May-2023

Publication Type: Journal Article Peer Reviewed: Y **Publication Status:** 1-Published
Journal: Science
Publication Identifier Type: DOI Publication Identifier: 10.1126/science.aba9192
Volume: 368 Issue: 6492 First Page #: 763
Date Submitted: 8/13/20 12:00AM Date Published: 5/1/20 4:00AM
Publication Location:
Article Title: Photocurrent detection of the orbital angular momentum of light
Authors: Zhurun Ji, Wenjing Liu, Sergiy Krylyuk, Xiaopeng Fan, Zhifeng Zhang, Anlian Pan, Liang Feng, Albert D
Keywords: orbital angular momentum
Abstract: Applications that use the orbital angular momentum (OAM) of light show promise for increasing the bandwidth of optical communication networks. However, direct photocurrent detection of different OAM modes has not yet been demonstrated. Most studies of current responses to electromagnetic fields have focused on optical intensity–related effects, but phase information has been lost. In this study, we designed a photodetector based on tungsten ditelluride (WTe2) with carefully fabricated electrode geometries to facilitate direct characterization of the topological charge of OAM of light. This orbital photogalvanic effect, driven by the helical phase gradient, is distinguished by a current winding around the optical beam axis with a magnitude proportional to its quantized OAM mode number. Our study provides a route to develop on-chip detection of optical OAM modes, which can enable the development of next-generation photonic circuits.
Distribution Statement: 2-Distribution Limited to U.S. Government agencies only; report contains proprietary info
Acknowledged Federal Support: **Y**

Publication Type: Journal Article Peer Reviewed: Y **Publication Status:** 1-Published
Journal: Light: Science & Applications
Publication Identifier Type: DOI Publication Identifier: 10.1038/s41377-020-00415-3
Volume: 9 Issue: 1 First Page #: 179
Date Submitted: 8/28/21 12:00AM Date Published: 10/1/20 4:00AM
Publication Location:
Article Title: Ultrafast control of fractional orbital angular momentum of microlaser emissions
Authors: Zhifeng Zhang, Haoqi Zhao, Danilo Gomes Pires, Xingdu Qiao, Zihe Gao, Josep M. Jornet, Stefano Lon
Keywords: fractional orbital angular momentum, carrier dynamics, ultrafast control
Abstract: On-chip integrated laser sources of structured light carrying fractional orbital angular momentum (FOAM) are highly desirable for the forefront development of optical communication and quantum information–processing technologies. While integrated vortex beam generators have been previously demonstrated in different optical settings, ultrafast control and sweep of FOAM light with low-power control, suitable for high-speed optical communication and computing, remains challenging. Here we demonstrate fast control of the FOAM from a vortex semiconductor microlaser based on fast transient mixing of integer laser vorticities induced by a control pulse. A continuous FOAM sweep between charge 0 and charge +2 is demonstrated in a 100?ps time window, with the ultimate speed limit being established by the carrier recombination time in the gain medium. Our results provide a new route to generating vortex microlasers carrying FOAM that are switchable at GHz frequencies by an ultrafast control pulse
Distribution Statement: 1-Approved for public release; distribution is unlimited.
Acknowledged Federal Support: **Y**

RPPR Final Report
as of 25-May-2023

Publication Type: Journal Article Peer Reviewed: Y **Publication Status:** 1-Published
Journal: Science
Publication Identifier Type: DOI Publication Identifier: 10.1126/science.abg3904
Volume: 372 Issue: 6540 First Page #: 403
Date Submitted: 8/28/21 12:00AM Date Published: 4/1/21 4:00AM
Publication Location:
Article Title: Higher-dimensional supersymmetric microlaser arrays
Authors: Xingdu Qiao, Bikashkali Midya, Zihe Gao, Zhifeng Zhang, Haoqi Zhao, Tianwei Wu, Jieun Yim, Ritesh A
Keywords: higher dimension, supersymmetric, microlaser, array
Abstract: The nonlinear scaling of complexity with the increased number of components in integrated photonics is a major obstacle impeding large-scale, phase-locked laser arrays. Here, we develop a higher-dimensional supersymmetry formalism for precise mode control and nonlinear power scaling. Our supersymmetric microlaser arrays feature phase-locked coherence and synchronization of all of the evanescently coupled microring lasers—collectively oscillating in the fundamental transverse supermode—which enables high-radiance, small-divergence, and single-frequency laser emission with a two-orders-of-magnitude enhancement in energy density. We also demonstrate the feasibility of structuring high-radiance vortex laser beams, which enhance the laser performance by taking full advantage of spatial degrees of freedom of light. Our approach provides a route for designing large-scale integrated photonic systems in both classical and quantum regimes.
Distribution Statement: 2-Distribution Limited to U.S. Government agencies only; report contains proprietary info
Acknowledged Federal Support: **Y**

Publication Type: Journal Article Peer Reviewed: Y **Publication Status:** 1-Published
Journal: Physical Review Letters
Publication Identifier Type: DOI Publication Identifier: 10.1103/PhysRevLett.126.163901
Volume: 126 Issue: 16 First Page #:
Date Submitted: 8/28/21 12:00AM Date Published: 4/1/21 4:00AM
Publication Location:
Article Title: Non-Hermiticity-Governed Active Photonic Resonances
Authors: Jose D.H. Rivero, Mingsen Pan, Konstantinos G. Makris, Liang Feng, Li Ge
Keywords: non-Hermitian, active photonic resonance
Abstract: Photonic resonances play an essential role in the generation and propagation of light in optical and photonic devices, as well as in light-matter interaction, including nonlinear optical responses. Previous studies in lasers and other open systems have shown exotic roles played by non-Hermiticity on modifying passive resonances, defined in the absence of optical gain and loss. Here we report a new type of resonances in non-Hermitian photonic systems that does not originate from a passive resonance, identified by analyzing a unique quantization condition in the non-Hermitian extension of the Wentzel-Kramers-Brillouin method. Termed active photonic resonances, these unique resonances are found in non-Hermitian systems with a spatially correlated complex dielectric function, which is related to supersymmetry quantum mechanics after a Wick rotation. Remarkably, such an active photonic resonance shifts continuously on the real frequency axis as optical gain increases.
Distribution Statement: 2-Distribution Limited to U.S. Government agencies only; report contains proprietary info
Acknowledged Federal Support: **Y**

RPPR Final Report
as of 25-May-2023

Publication Type: Journal Article Peer Reviewed: Y **Publication Status:** 1-Published
Journal: Nature
Publication Identifier Type: DOI Publication Identifier: 10.1038/s41586-022-05339-z
Volume: 612 Issue: 7939 First Page #: 246
Date Submitted: 5/18/23 12:00AM Date Published: 11/1/22 4:00AM
Publication Location:
Article Title: Spin–orbit microlaser emitting in a four-dimensional Hilbert space
Authors: Zhifeng Zhang, Haoqi Zhao, Shuang Wu, Tianwei Wu, Xingdu Qiao, Zihe Gao, Ritesh Agarwal, Stefano
Keywords: spin-orbit microlaser, high-dimensional superposition, Hilbert space
Abstract: Here we demonstrate a hyperdimensional, spin–orbit microlaser for chip-scale flexible generation and manipulation of arbitrary four-level states. Two microcavities coupled through a non-Hermitian synthetic gauge field are designed to emit spin–orbit-coupled states of light with six degrees of freedom. The vectorial state of the emitted laser beam in free space can be mapped on a Bloch hypersphere defining an SU(4) symmetry, demonstrating dynamical generation and reconfiguration of high-dimensional superposition states with high fidelity.
Distribution Statement: 1-Approved for public release; distribution is unlimited.
Acknowledged Federal Support: **Y**

DISSERTATIONS:

Publication Type: Thesis or Dissertation
Institution: University of Pennsylvania
Date Received: 13-Aug-2020 Completion Date: 12/31/19 3:54PM
Title: Non-Hermitian Topological Photonics: From Concepts to Applications
Authors: Zhao, Han
Acknowledged Federal Support: **N**

Partners

,

I certify that the information in the report is complete and accurate:
Signature: Liang Feng
Signature Date: 5/18/23 2:27PM

Thrust I: Non-Hermitian interaction for active control of topological insulating phase

Discovered by Kane and Mele, topological insulators represent a new class of materials, providing robust and defect-free edge channels for carrier transport (such as electrons and photons). Flexibly reconfiguring topological light pathways can enable a completely new paradigm for high-density photonics routing, sustaining the growing demand for data capacity. However, the desired topological robustness unfortunately backfires to destroy the hope of topological tunability: redefining topological light pathways requires considerable perturbations to drive the topological phase transition inside the bulk structure that are exceptionally difficult to access in integrated photonic chips. Such a severe limitation prevents photonic topological insulators from being practically applied, since the topological mode only exists at the static structural boundary/interface so that most of the footprint of the photonic structure is unutilized.

Now, we have overcome this fundamental limitation and demonstrated arbitrary robust light steering (Fig. 1). A new topological light transport channel is created via non-Hermitian control on an active photonic platform within the bulk of an otherwise Hermitian photonic topological insulator with uniform topological property. Non-Hermitian control is conducted by optically pumping the photonic lattice to create distributed gain (via external pumping) and loss (intrinsic material loss without pumping) domains (Fig. 1A). The emergence of new topological states is observed at the boundary of the gain and loss domains when the local non-Hermiticity (i.e. the gain/loss contrast) is driven across a quantum exceptional point (EP). Instead of "battling" against topological protection, we perform non-Hermitian control to enable a new kind of topological states to actively steer the topological light on-demand via projecting the designed spatial pumping patterns onto the topological photonic lattice (Fig. 1B).

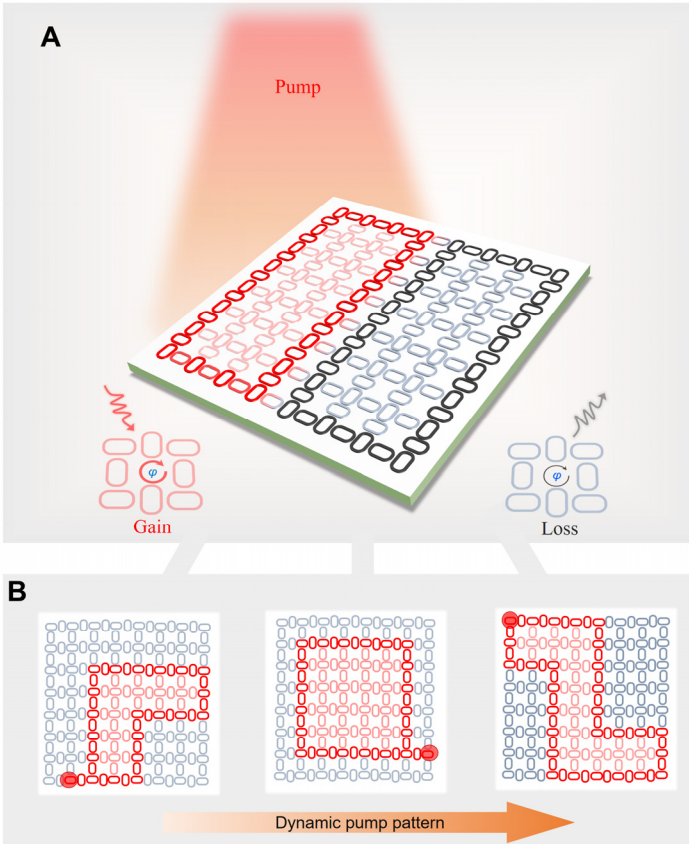

Figure 1. Non-Hermitian control of light propagation in a topological microring lattice. (**A**) Scheme of the pump-induced local non-Hermitian symmetry breaking, which creates new topological edge channels along the gain/loss interface in the bulk of the photonic lattice with uniform global topology defined by the same geormetric phase φ in the gain (red) and loss (black) plaquettes. **(B)** The topological edge states can be dynamically reconfigured to steer light along any boundaries defined by the arbitraririly patterned pump beam.

The emergence of new topological states is observed at the boundary of the gain and loss domains when the local non-Hermiticity (i.e. the gain/loss contrast) is driven across the

non-Hermitian parity-time symmetric phase transition point, i.e. exceptional point (EP) (Fig. 2).

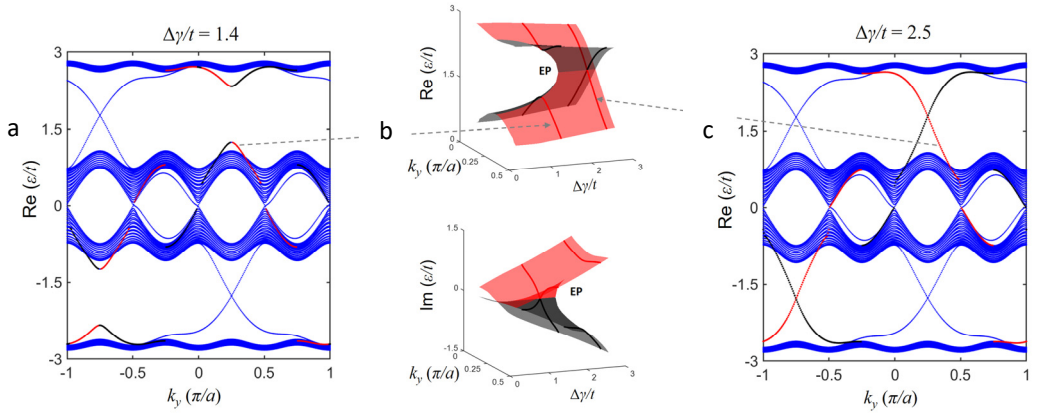

Figure 2. **Emergence of topological interface state via non-Hermitian phase transition.** (a) Calulated band structure for $\Delta\gamma = (\gamma_1 - \gamma_2) = 1.4t$ and $\varphi = \pi/2$. (b) Riemann sheets of the real and imaginary parts of the eigenspectrum, with varying gain/loss contrast and momentum, near the EP degeneracy at ($k_y = 0.25\pi/a$, $\Delta\gamma = 1.785t$, $\gamma_1 = -\gamma_2$) in the upper bandgap. (c) Band structure for $\Delta\gamma = 2.5t$ showing two new anti-crossing protected interface states which counterpropagate at the gain/loss boundary of the lattice. In addition to the edge states at the physical boundaries (blue curves in the gaps), emergence of two dispersive pseudo edge states from the bulk bands are shown near the EP degeneracies at $k_y = 0.25\pi/a$ (upper band) and $k_y = -0.75\pi/a$ (lower band). These two states are highlighted one with red and other with black color inside the lower bandgap.

In contrast to previously studied topological states confined only at the static boundary/interface of the structure, the new non-Hermitian-controlled topological state can enable robust transmission links inside the bulk. Consequently, guided light can be directed along any arbitrary pathway according to the pumping patterns generated from a spatial light modulator, fully utilizing the entire footprint in topologically routing optical signal to any desired output port (Fig. 3).

Owing to the fully utilized footprint, the increased input-output connections in our system can be flexibly configured by the programmed actively-control patterns, avoiding any crossing nodes and therefore minimizing crosstalk and signal loss. The ports-to-footprint ratio is at least >2 orders of magnitude compared to the state-of-the-art photonic routers/switches, therefore leading to high impact on the large-information capacity applications (e.g. 5G or even 6G networks). Moreover, the ultra-flexible nature of our topological light control is general and applies to other topological materials. The achievable

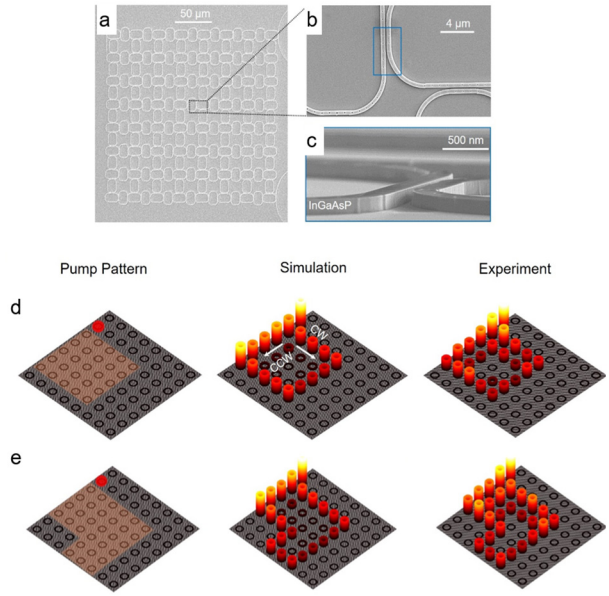

Figure 3. **Reconfigurable topological routing of light. (a)-(c):** A photonic topological insulator consisting of coupled microrings. (d),(e) show the reconfigured topological transmission links along the gain/loss interface that can be reconfigured via controlling optical pumping patterns (orange regions), coupled with a lasing site ring (denoted by red dots).

functions can cover a large variety of photonic components and networks beyond light steering and routing, thereby promising for the development of integrated photonic circuitry for high-density data processing.

References:

Han Zhao, Xingdu Qiao, Tianwei Wu, Bikashkali Midya, Stefano Longhi, and Liang Feng, "Non-Hermitian topological light steering," Science 365, 1163-1166 (2019).

Thrust II: Non-Hermitian interaction through imaginary valued gauge field

Here, we demonstrate that the strategy of non-Hermitian controlled single chiral vortex lasing can be generalized for multiple vortex generation in a scalable way by harnessing the concept of imaginary gauge fields. For demonstration, we have designed and experimentally characterized integrated microring laser system capable of emitting two vortices of desirable chirality. We consider the two-microring system with two control waveguides between them shown in Fig. 4. This coupled system in the linear regime of operation is governed by the following Hamiltonian:

$$H = \begin{pmatrix} \omega_{\circlearrowright}^{L} & 0 & \kappa e^{-\gamma} e^{+\gamma_B} & 0 \\ 0 & \omega_{\circlearrowleft}^{L} & 0 & \kappa e^{-\gamma} e^{+\gamma_T} \\ \kappa e^{-\gamma} e^{+\gamma_T} & 0 & \omega_{\circlearrowright}^{R} & 0 \\ 0 & \kappa e^{-\gamma} e^{+\gamma_B} & 0 & \omega_{\circlearrowleft}^{R} \end{pmatrix}$$

where $\omega_{\circlearrowright/\circlearrowleft}^{L/R}$ denotes the $\circlearrowright/\circlearrowleft$ resonance of WGM mode in left/right ring respectively, κ denotes the coupling of modes between two different rings without any gain or loss control, $-\gamma$ is the single-pass attenuation from the intrinsic material loss, and $+\gamma_T$ / $+\gamma_B$ are the optical amplification from the top/bottom waveguides, respectively. An unbalanced amplification in the upper and bottom arms provides asymmetric coupling between either clock-wise or counter-clock-wise modes in the two rings, corresponding to an effective imaginary gauge field $h = \frac{\gamma_B - \gamma_T}{2}$. The dual ring system is designed with the same ring/waveguide geometrical parameters as the single ring system.

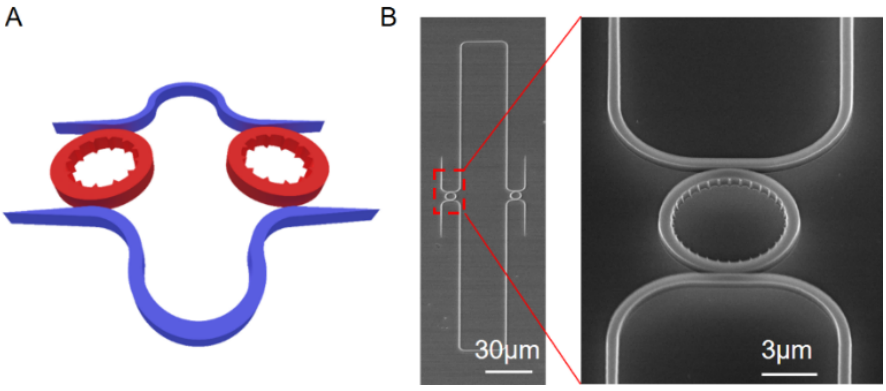

Figure 4. **Schematic design and SEM pictures of a two microring OAM lasers.** (A) Two microrings coupled with each other through two waveguide control arms that implement a synthetic imaginary gauge field, i.e. asymmetric mode coupling. Modes in the two rings with equal oscillation directions can couple with each other (i.e. the $\circlearrowright/\circlearrowleft$ modes couple with $\circlearrowright/\circlearrowleft$ modes, respectively). Unbalanced gain in upper and lower control waveguide arms yields asymmetric mode coupling. (B) SEM pictures of a fabricated laser system. Microring radius is 3.5 μm, width is 0.65 μm and height is 200 nm. $M = 32$ periodic scatters are patterned at the inner sidewall of the microring and WGM order $N = 32$.

Without external pumping, i.e. for γ_T=γ_B=0, the coupling strength of the modes between different rings is again negligible due to the high intrinsic material loss γ. As such, $\circlearrowright$ and $\circlearrowleft$ modes can coexist with equal amplitude in both microring resonators, resulting in a zero net OAM charge as shown in Fig. 5A. When the upper control waveguide is pumped (γ_T>0, γ_B=0),

an effective non-vanishing imaginary gauge h is realized and optical gain overcomes the intrinsic material loss and introduces a net gain around $50\ \mathrm{cm}^{-1}$ (i.e. $\kappa e^{-\gamma} e^{+\gamma_T} = 125.5\ \mathrm{GHz}$). As a result, the coupling from the $\circlearrowright^L$ mode to the $\circlearrowright^R$ mode ($125.5\ \mathrm{GHz}$) is much greater than the back coupling ($\sim 0\ \mathrm{Hz}$). Simultaneously, the coupling from the $\circlearrowleft^R$ mode to the $\circlearrowleft^L$ mode ($125.5\ \mathrm{GHz}$) is much greater than the back coupling ($\sim 0\ \mathrm{Hz}$). The eigenvector of the Hamiltonian is therefore $[\circlearrowright^L \quad \circlearrowleft^L \quad \circlearrowright^R \quad \circlearrowleft^R]^T = [0 \quad 1 \quad 1 \quad 0]^T$, which corresponds to unidirectional lasing of $\circlearrowleft/\circlearrowright$ modes in left/right ring resonators (Fig. 5B). In contrast, when the bottom control waveguide is pumped the gauge field h is reversed, resulting in lasing with opposite chirality shown in Fig. 5C.

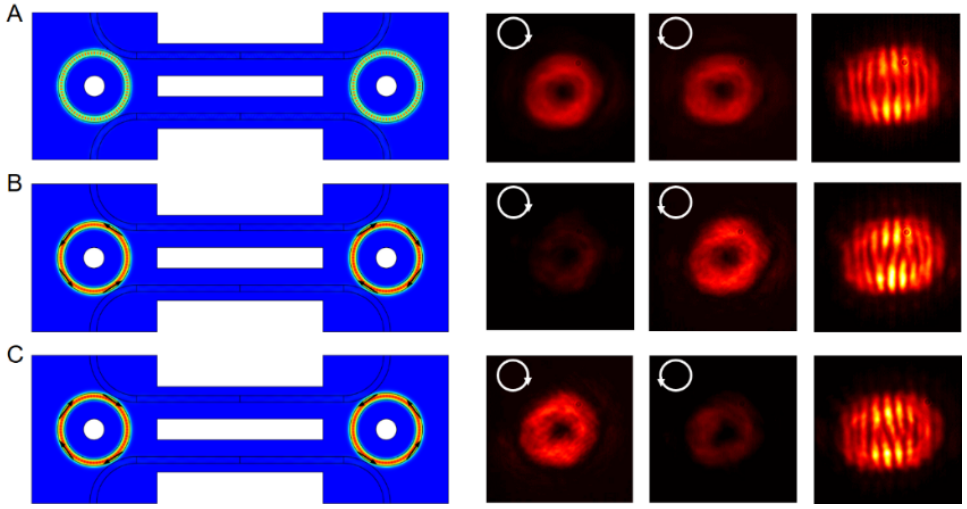

Figure 5. Characterization of chirality tuning of two OAM microlaser system. (A) None of the two control arms were pumped (i.e. $h = 0$), and emission was captured from the left-side ring laser only. The right hand circular polarized component is about equal to the left hand circular polarized component. Off-center self-interference shows no fork. (B) The upper control arm was pumped (i.e. $h < 0$) and caused lasing with $\circlearrowleft$ mode in the left-side ring and $\circlearrowright$ mode in the right-side ring. The left-hand circularly polarized component was dominant in the left-side ring emission. Off-center self-interference shows a pair of forks where one fringe split into two. (C) The lower control arm was pumped (i.e. $h > 0$) and caused lasing that has opposite chirality to panel (B) behavior. The right-hand circular polarized component is dominant in the left-side ring emission. Off-center self-interference also shows a pair of forks where one fringe split into two but in the opposite direction of (B) forks.

Moreover, we further developed the actively controlled non-Hermitian gauge to allow for simultaneous manipulations of both amplitude and phase, by which we demonstrated a hyperdimensional (i.e., high-dimensional superposition), spin-orbit microlaser for chip-scale flexible generation and manipulation of arbitrary four-level states. Two microcavities coupled through a non-Hermitian synthetic gauge field are designed to emit spin-orbit-coupled states of light with six degrees of freedom. The vectorial state of the emitted laser beam in free space can be mapped on a Bloch hypersphere defining an SU(4) symmetry, demonstrating dynamical generation and reconfiguration of high-dimensional superposition states with high fidelity. The ability to conveniently generate and reconfigure arbitrary high-dimensional superposition states not only significantly expands information capacity, but also enhances noise tolerance and information security, thereby promising for next-generation information science and technology photonics infrastructure.

Here, we strategically designed non-Hermitian coupling between microring cavities (**Fig. 6a**) to provide a flexible control of up to six control parameters, thus enabling to cover, in principle, the full 4D Hilbert space. Each microring intrinsically supports two degenerate modes (CW and CCW). The geometry of the cross-section of the microring resonator is designed to support on-chip spin-orbit locking: left-hand ($\uparrow$: spin-up with s = +1) or right-hand ($\downarrow$: spin-down with s = –1) polarization in the evanescent tail of guided mode is locked to only one chiral mode (either CW or CCW). The angular gratings of coupled laser cavities are designed to generate the spin-orbit locked states $|l, s\rangle$ of laser radiations in the far field, corresponding to CW/CCW modes in two coupled cavities: $|+2,\uparrow\rangle$ (CW) and $|-2,\downarrow\rangle$ (CCW) from the left ring and $|-2,\uparrow\rangle$ (CW) and $|+2,\downarrow\rangle$ (CCW) from the right ring, each featuring an individual HOPS. Therefore, the entire coupled laser system can be viewed as a four-level system with two coupled HOPS. As a result, a four-dimensional Bloch hypersphere is formed in the laser emission, featuring high-dimensional spin-orbit entanglement. Note that the four spin-orbit-coupled states also have exactly the same propagation constant, and hence they overlap completely also in time. Furthermore, they share the same diffraction and modal conversion (from free space to fibers and vice versa), and can carry the same self-healing properties. Consequently, these states can maintain their coherence after long-distance propagation, which is critical for long-haul communications.

Furthermore, we show the ability to arbitrarily generate any superposition state in this 4D space. By selective pumping and phase tuning of the control waveguides, we realize not only delicate manipulation of optical chirality, but also precise maneuvering of the relative phase between CW and CCW modes in each microring, preparing the spin-orbit entangled states on two HOPS at will, for example, the full phase control along the longitude and reconfiguration of

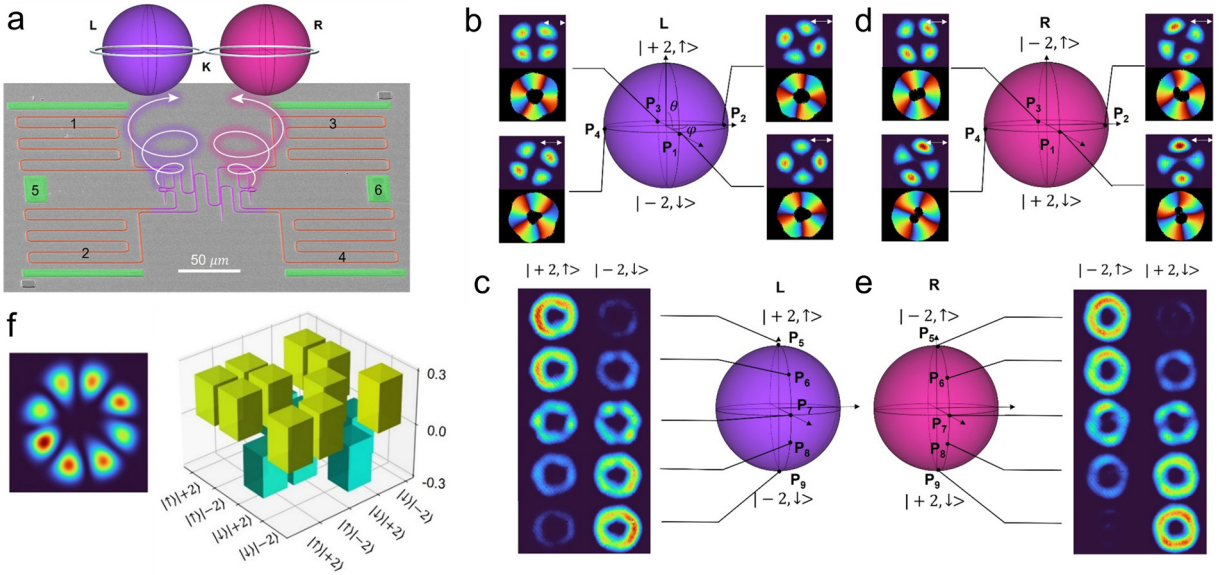

Figure 6. (a) Hyperdimensional spin-orbit microlaser for the generation of high-dimensional classical entanglement superposition states. (b) and (c) show the phase and amplitude control on HOPS L to move the state in the longitude and latitude, respectively. (d) and (e) show the phase and amplitude control on HOPS R, respectively. (f) The generated 4D graph state and its experimentally characterized density matrix, featuring the high-dimensional spin-orbit classical entanglement.

the superposition state along the latitude of HOPS **L** (**Figs. 6b** and **6c**). Similar control can be independently performed in the right microring to prepare the superposition state along the longitude and latitude of HOPS **R** (**Fig. 6d** and **Fig. 6e**). Additionally, the relative amplitude and phase between HOPS **L** and **R** can be controlled by onsite frequency detuning and adjusting gain/loss contrast between two microrings, providing two additional control parameters to realize a full 4D Hilbert space. Moreover, the coupling of HOPS **L** and **R** on HOPS **K** (**Fig. 6a**) via the non-Hermitian gauge, while each representing a distinct SU(2) group, enables the generation of the high-dimensional superposition states that cover the entire 4D Hilbert space. With the full control over the six DOFs discussed above, the tuning operations involved contain a representation of the SU(4) group.

More remarkably, the ability to map the vectorial states in a full 4D space enables the generation and reconfiguration of intriguing high-dimensional superposition states with high fidelity, including unique graph states that are resilient to noise, and therefore, important in computations and communications for error corrections. For example, **Figure 6f** demonstrates the generation of an iconic state: $|\psi_1\rangle = \frac{1}{2}(|+2,\uparrow\rangle + |-2,\downarrow\rangle + |-2,\uparrow\rangle - |+2,\downarrow\rangle)$, a high-dimensional spin-orbit graph state corresponding to in-phase superposition of state P1 on HOPS L and state P3 on HOPS R. Opposite polarization windings from the two rings (see the phase winding maps in Figs. 1b and 1d) yield a cross-correlation pattern with 8 lobes in the far field, where high/low intensity denotes aligned/orthogonal polarizations, respectively, arising from the vectorial nature of the spin-orbital graph state. Furthermore, the experimentally measured density matrix shows a high fidelity of 0.998, in great agreement with the calculated result.

References:

Zhifeng Zhang, Xingdu Qiao, Bikashkali Midya, Kevin Liu, Jingbo Sun, Tianwei Wu, Wenjing Liu, Ritesh Agarwal, Josep Miquel Jornet, Stefano Longhi, Natalia M. Litchinitser, and Liang Feng, "Tunable topological charge vortex microlaser," Science 368, 760-763 (2020).

Zhifeng Zhang, Haoqi Zhao, Shuang Wu, Tianwei Wu, Xingdu Qiao, Zihe Gao, Ritesh Agarwal, Stefano Longhi, Natalia M. Litchinitser, Li Ge, and Liang Feng, "Spin-orbit microlaser emitting in a four-dimensional Hilbert space," Nature 612, 246-251 (2022).

Thrust III: Non-Hermitian interaction through optical reservoirs

The nonlinear scaling of complexity with the increased number of components in integrated photonics is a major obstacle impeding large-scale phase-locked laser arrays. Control of mutual coupling is thus the key to phase-locking of all the elements and further driving them to function collectively. Here, following the supersymmetric principle, we design dissipative superpartner arrays that function as an optical reservoir to couple with the main laser array under the parity-time symmetric condition to enforce phase-locking and to enable coherent oscillation in a two-dimensional (2D) laser array of evanescently coupled microlasers (Fig. 7a), opening new avenues for the realization of integrated high-radiance sources.

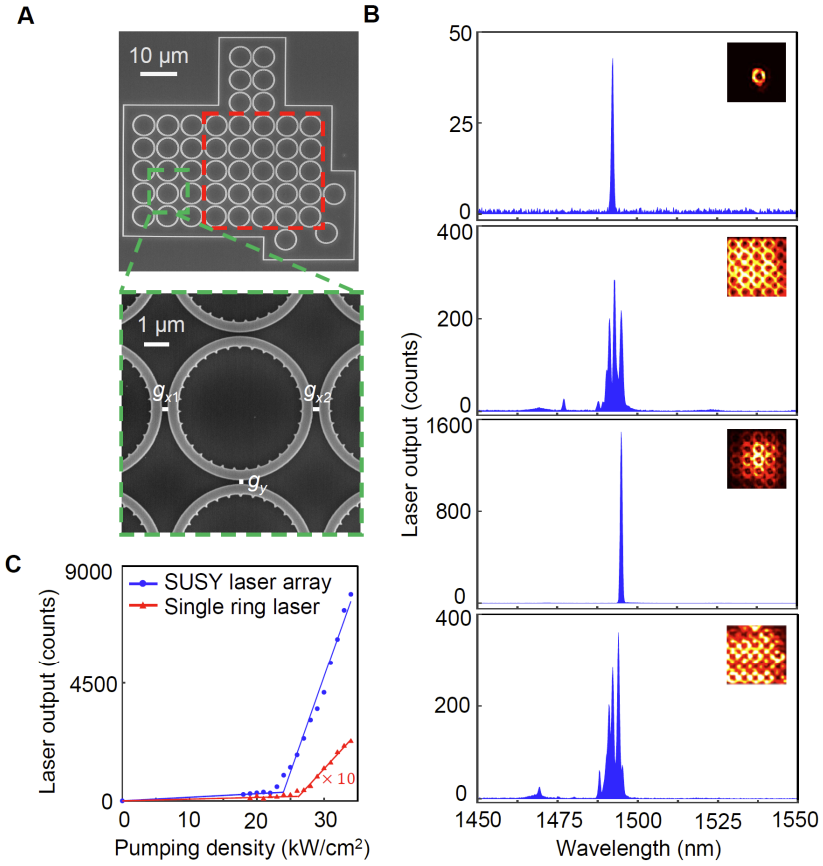

Figure 7. Experimental characterization of the higher dimensional supersymmetric optical array. (**A**) SEM images of the SUSY optical array. The main array is denoted by the red box, evanescently coupled to the supersymmetric and auxiliary partners. (**B**) Emission spectra, from top to bottom, of a single microring laser (single frequency lasing at 1492 nm), a 5×5 array of microring lasers with identical design parameters but no coupled supersymmetric and auxiliary partners, the supersymmetric microlaser array coupled with dissipative partners by selective pumping (single frequency lasing at 1495 nm), and the supersymmetric microlaser array but with uniform pumping on both the main array and partners, respectively, at the same pumping intensity of 32 kW/cm^2. (**C**) Light–light curve showing the lowering of the threshold and enhancement of emission output (the slope efficiency) in the SUSY optical array compared to a single microring.

In this scheme, the spectrum of superpartners (i.e., the optical reservoir for the main array) is identical to the main array apart from the fundamental in-phase supermode. Strategically

controlled coupling of the main array with its dissipative superpartners and auxiliary partner microrings, by matching both the eigen-frequencies and mode distributions, ensures the suppression of all but the fundamental transverse supermode, yielding efficient single-supermode lasing (Fig. 7b). Our experiment shows all 25 individual microlasers in the main array oscillate and contribute to power enhancement with a factor of ~25 with respect to emission from a single microlaser, as evidently shown by the light-light curves where the slope efficiency of the SUSY microlaser array is 26.3 times higher than that of a single microlaser (Fig. 7c). Additionally, the SUSY microlaser array also exhibits a lower lasing threshold because of better optical modal overlap with the gain material.

Beyond power enhancement, the major virtue of the higher-dimensional in-phase supermode emission is the strong 2D concentration of its emission in the far field, with ultimate energy density quadratically growing with the number of arrayed elements. The far-field pattern of the emission beam is a product of far-field diffraction of the supermode and single microring emission (Figs. 8a). As the designed angular grating meets the condition for equi-phase emission, emissions from all scatterers in the single ring add constructively at the center of the far field as they carry the same polarization (Fig. 8b). Specifically, the emission from the 2D SUSY array exhibits beam divergence of ~2°, compared to a single microring of ~11° with more than two orders of magnitude enhanced in energy density (Figs. 8c and 8d).

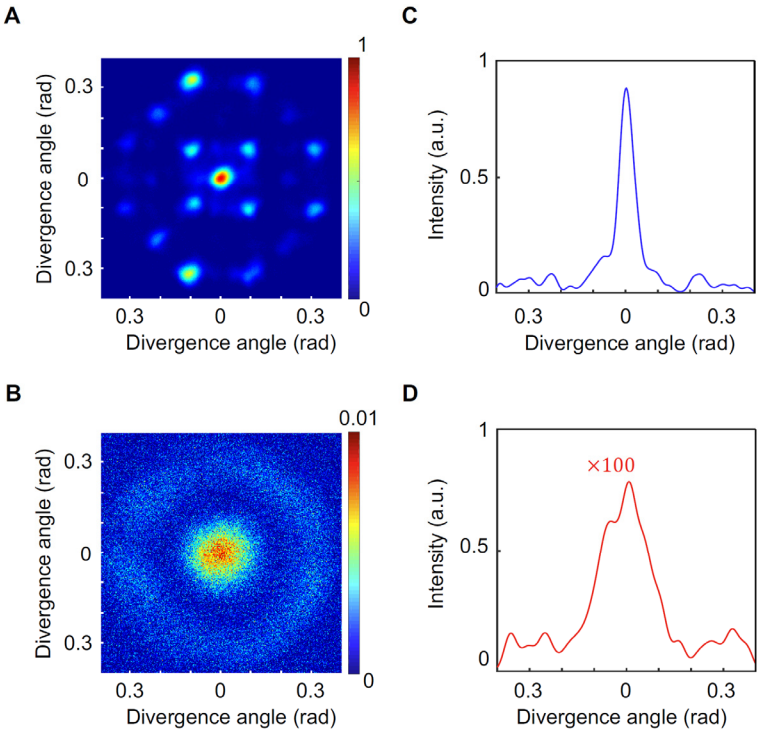

Figure 8. Far-field characterization of laser emission from the higher-dimensional supersymmetric optical array. (**A**) and (**B**) are far-field diffraction patterns of emissions from the SUSY array and a single microring, respectively. (**C**) and (**D**) are the corresponding intensity distribution of emissions from the SUSY array and single microring, respectively, both along the *x* axis, showing small divergence of ~2° (vs. divergence of ~11° for the single microring) and energy concentration with 2 orders of magnitude enhancement in intensity associated with the emission from the SUSY microlaser array.

References:

Xingdu Qiao, Bikashkali Midya, Zihe Gao, Zhifeng Zhang, Haoqi Zhao, Tianwei Wu, Jieun Yim, Ritesh Agarwal, Natalia M Litchinitser, and Liang Feng, “Higher-dimensional supersymmetric microlaser arrays,” Science 372, 403-408 (2021).